

# Delineation by seismic attribute algorithms of fracture patterns in a 3D GPR volume

Oswaldo Davogustto\*, University of Oklahoma, USA

Roger A. Young, University of Oklahoma, USA

Ibrahim Cemen, Oklahoma State University, USA

## Summary

Fractures are caused by changes in stress patterns. The main objective of this study is to delineate and map fractures in a granitic body with the help of attribute algorithms. The data is a 3D GPR survey consisting of 24 parallel lines. Changes in the dielectric constant between the granite and the fracture fill (air or water) will produce a distinctive amplitude fracture response. Amplitude attribute algorithms allow the identification of fracture patterns. The resulting fracture interpretation is corroborated by the surface fracture data.

## Introduction

Seismic attributes are defined as any measurement derived from seismic data (Sheriff, 1991). Uses of an attribute algorithm on GPR reflection data have shown that attributes are a powerful tool for radar interpretation (e.g., Young et al., 1997, Moysey et al 2006 Geerdes et al, 2007, McClymont et al, 2008), yet the tools remain underutilized. The main objective of this study is to define fracture planes in a 3D GPR data set using attribute algorithms and outcrop fracture measurements. We have acquired a 3D GPR survey at the intrusive Tishomingo Granite in the Arbuckle Mountains in southern Oklahoma (Figure 1).

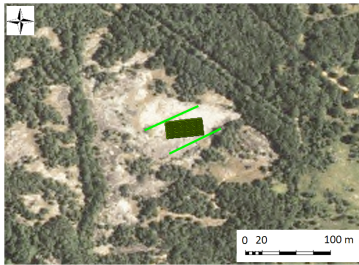


Figure 1. 3D GPR survey area superimposed in satellite photo. Green lines show surface recognized trends that are associated with fractures.

## Data Processing

Three stages of processing were required before attribute calculation: first stage was balancing the amplitudes in the data. The second stage was applying a local interactive 2D  $f$ - $k$  band pass filter for airwave removal. Then third step comprises merge and 3D geometry definition, AGC, phase shift migration and static corrections (Figures 2).

## Data Interpretation

Even after careful processing of the data, the identification of fractures in the data was not obvious. This situation was not helped by interpretation of *individual* 2D vertical slices. What was needed was a *volume*-based attribute evaluated at every point and an interpretation system that allows three-dimensional visualization of an interpreted surface. Such attribute algorithms are widely used in the oil industry for detection and delineation of stratigraphic and structural features in seismic data. The keystone in the attribute theory is that they quantify a volume-based statistical measure of the amplitude, the frequency, or even the phase of the data (Marfurt, personal communication, 2008). Based on this idea we applied two different types of attribute algorithms to the data volume, most negative curvature and Ant Tracking<sup>TM</sup>. Most Negative Curvature and Ant Tracking<sup>TM</sup> results are shown in Figures 3 and 4 respectively. Most negative curvature enhances the trends that have a more N-S and E-W orientation. Ant Tracking was applied to the curvature results for fracture pattern enhancement (Pedersen et. al., 2006) showing a predominant a feature with E-W trend is most distinctive followed by several N-S patterns. The fracture interpretation was made the combining multiple vertical sections with the Ant Tracking time slice. For each vertical section a fracture trend was picked displaying a time value (color scaled sticks on figures 5 – 7). This time –color scale display also gives a sense of dip for each fracture. The result was an identification of 9 fracture planes shown in different perspectives in Figures 5 - 7.

## Conclusions

Volumetric attribute analysis for 3D GPR data is a powerful tool for interpretation. This work demonstrates that fracture interpretation is facilitated with the aid of attribute algorithms. Attribute – determined fracture directions correlate with the orientation of geologically mapped lineaments. 3D attributes determine spatial orientation of fractures. Shape attributes such as curvature help to delineate fracture patterns and Ant Tracking<sup>TM</sup> enhances trends and helps to delineate fracture patterns.

## Acknowledgements

We wish to thank Sensors and Software, Parallel, Schlumberger, Oklahoma Water Resources Research, Noel Osborn, Mr. John Bruno, Dr. Kurt J. Marfurt and Tim Kwiatkowski, Carlos Russian, Tim Sickbert, Andrea Miceli, Ha Mai and Kui Zhang also for their help.

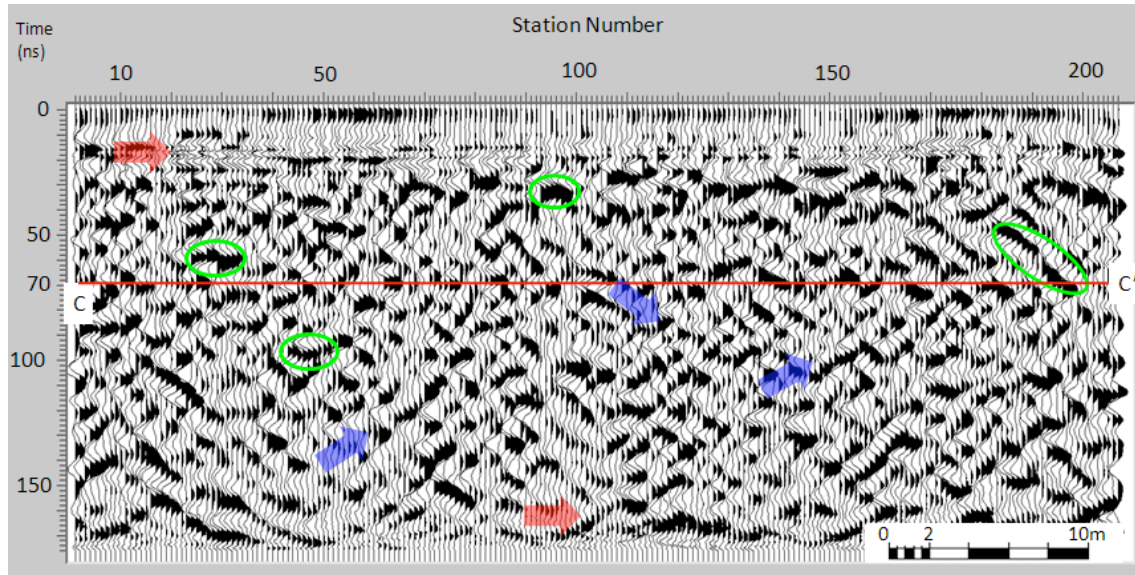


Figure 2. Inline 15 processed. The air wave was successfully removed using a local interactive 2D  $f$ - $k$  band pass filter. The amplitude energy has been balanced with AGC and the diffractions were partially collapsed using phase shift time migration. The green circles show the diffractors. Blue arrows show trends that could be associated with fractures. C-C' is a time section trough 70 ns. Red arrows show processing artifacts.

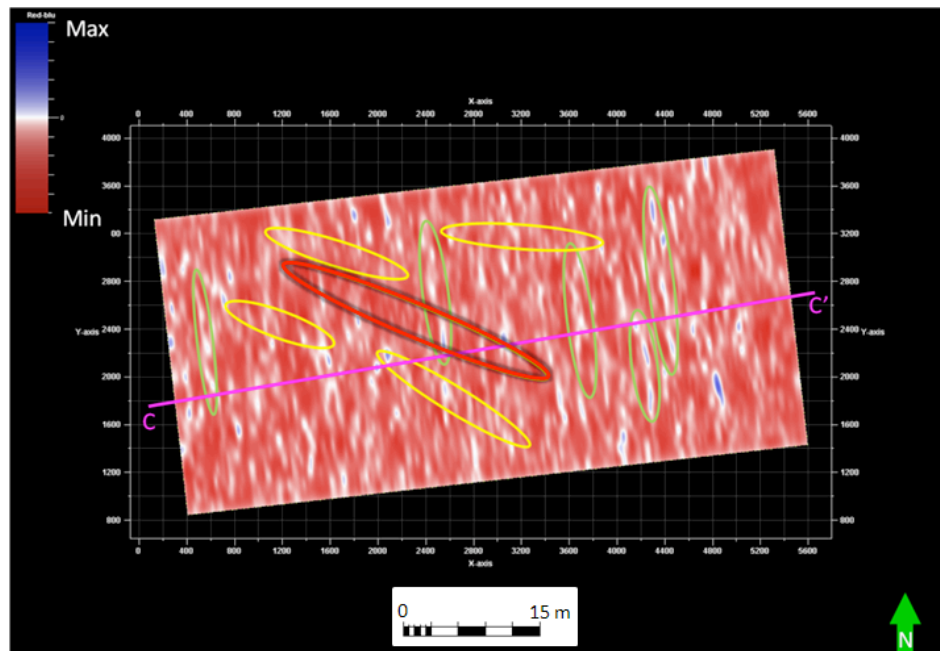


Figure 3. Time slice trough Most Negative Curvature at 70 ns. The zero curvature patterns for this algorithm align in a N-S trend mostly (green circles). Also some NW-SE trends are seen (yellow circles), but not as clearly as the N-S.

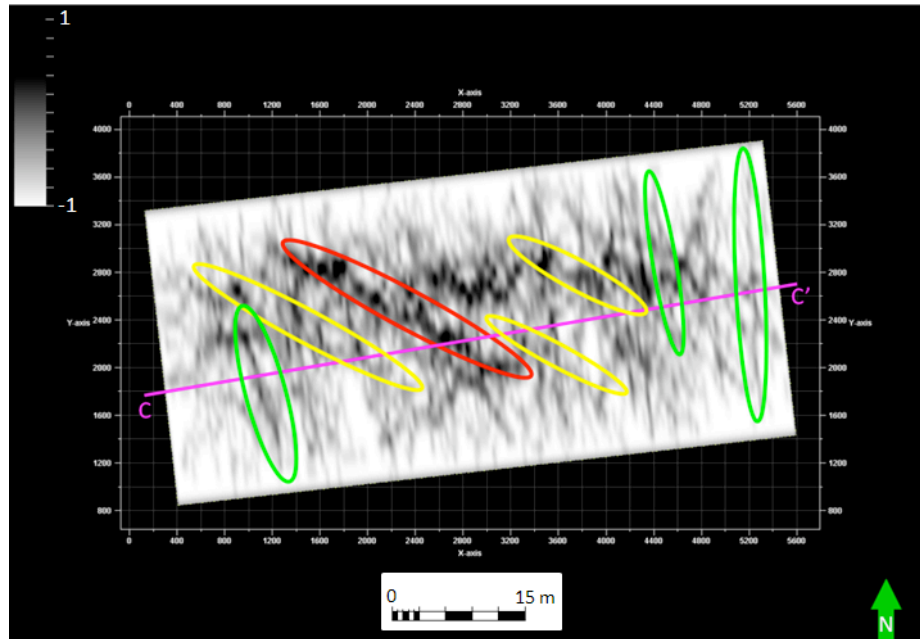


Figure 4. Time slice trough Ant Tracking on Most Negative Curvature at 70 ns, the Ant Tracking algorithm enhances the features detected by other attributes. The black trends are associated with discontinuities on the reflector character that can be correlated with fractures but some can be also due to artifacts of the algorithms. The two major trends observed are a N-S (green circles) trend and a NW-SE trend (yellow circles). The red circle shows the NW-SE trend with a strong response to ant tracking.

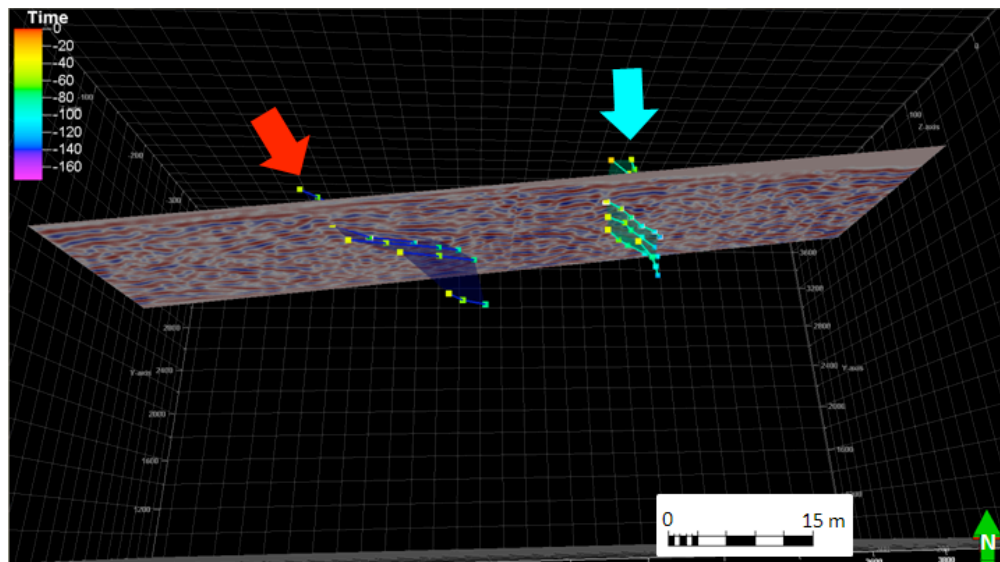


Figure 5. Fracture interpretation in 3D view. For the fracture interpretation time sections were evaluated and trends that were recognized as fractures were picked, red and cyan arrows point fracture interpretation. The orientation of the section is SW – NE.

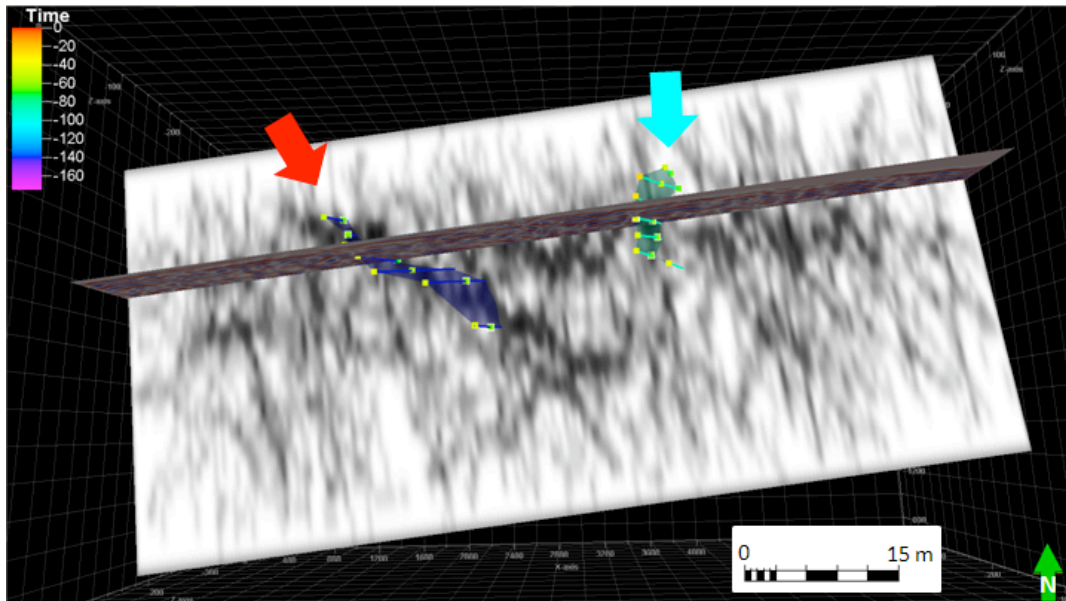


Figure 6. Fracture interpretation in 3D view. The combination of Ant Tracking time slice and vertical sections made easier the identification of fracture patterns in the data. Notice that the fracture planes shown in figure 5 also correspond to trends enhanced by the Ant Tracking attribute, red and cyan arrows point fracture interpretation. The time slice is seen from above and intersecting with the inline 15.

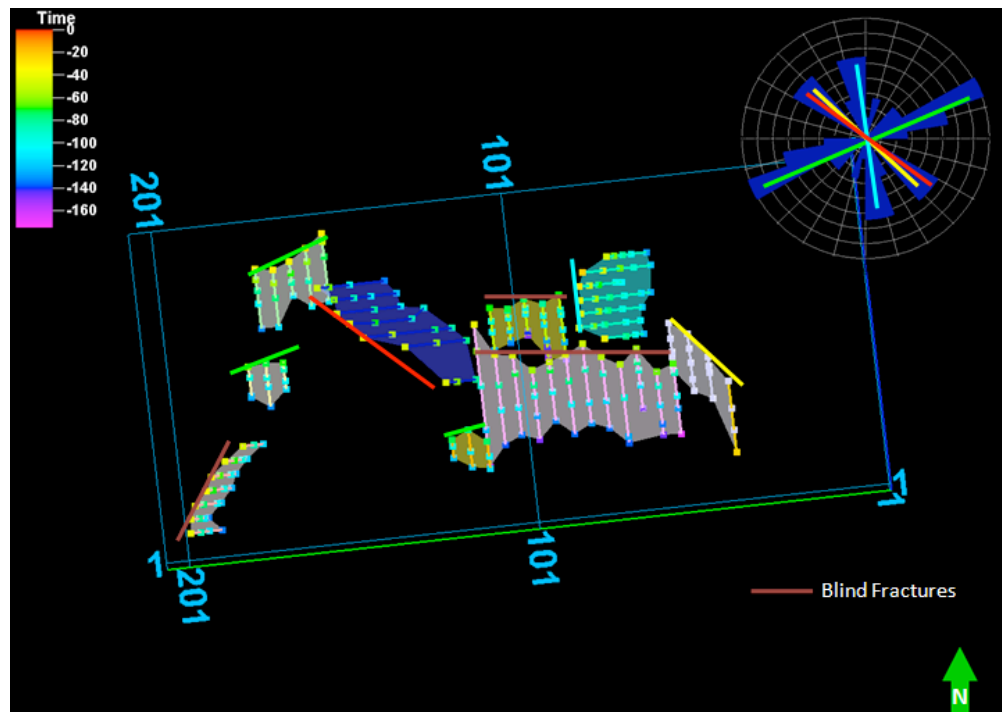


Figure 7. Comparison of fracture interpretation with mapped surface fractures (rose diagram, top right). Each fracture azimuth has been highlighted with a colored line in order to make the comparison. Red and Cyan trends are also examples in figures 5 and 6. Nine fractures were interpreted by combining time sections and volume attributes. Fractures that are not following any trend seen in surface are interpreted as blind fractures. This figure is a projection of the fracture interpretation on to the time slice at zero time.